Journal of Fluids and Structures (2001) **15,** 23–37
doi:10.1006/jfls.2000.0323, available online at http://www.idealibrary.com on IDEAL®

FEEDBACK CONTROL OF VORTEX SHEDDING FROM A CIRCULAR CYLINDER BY ROTATIONAL OSCILLATIONS

N. Fujisawa

Department of Mechanical and Production Engineering, Niigata University 8050 Ikarashi 2, Niigata 950-2181, Japan

Y. Kawaji and K. Ikemoto

Department of Mechanical System Engineering, Gunma University, Kiryu 376, Japan

(Received 30 June 1999, and in final form 6 June 2000)

The present paper describes a new active method for controlling vortex shedding from a circular cylinder in a uniform flow at medium Reynolds numbers. It uses rotary cylinder oscillations controlled by the feedback signal of a reference velocity in the cylinder wake. The effectiveness of this feedback control is evaluated by measuring the response of mean and fluctuating velocities in the cylinder wake, the spanwise correlation, the power spectrum, and the fluid forces acting on the cylinder. It is found that the velocity fluctuations and the fluid forces are both reduced by the feedback control with optimum values of the phase lag and feedback gain. The simultaneous flow visualization synchronized with the cylinder oscillation indicates the attenuation as well as the mechanisms of vortex shedding under the feedback control, which is due to the dynamic effect of cylinder oscillation on the vortex formation.

1. INTRODUCTION

Vortex streets are formed in the wake of a bluff body over a wide range of Reynolds numbers. The physics of vortex formation and the wake structure have been the topics of research for many years and have been studied by many researchers. It is well known that the strength of the vortices is increased when the natural frequency of the structure in a stream approaches the frequency of the vortex shedding. This phenomenon is known as resonance or synchronization and has been the topic of research related to the engineering problems of flow-induced vibration and noise. The outcomes of such studies are summarized in some review papers by Sarpkaya (1979), Bearman (1984), Griffin & Hall (1991), and others. Nowadays, passive methods for attenuating the vortex shedding, called vortex suppression devices, such as the axial slats, the splitter plate, the helical strake and others, have been developed through *ad hoc* experiments. These devices were applied to solve problems in wind and marine engineering. Such devices act by disrupting or preventing the formation of an organized two-dimensional structure of vortex shedding. The details about the passive methods are described by Blevins (1990).

On the other hand, active methods for controlling the vortex shedding from a circular cylinder have been investigated in recent years by Baz & Ro (1991), Huang (1996), and Gunzburger & Lee (1996). However, the number of studies is very small compared with those of the passive controls. Okajima *et al.* (1975), Taneda (1978) and Filler *et al.* (1991)

0889–9746/01/010023 + 15 $35.00/0

studied the effect of rotary oscillations of a circular cylinder at relatively low Reynolds numbers. They demonstrated the possible modification of vortex shedding and found that the extent of cylinder peripheral speeds which affected the vortex shedding was smaller than 3% of the free-stream velocity. The aerodynamic performance of rotationally oscillating cylinder at medium Reynolds number ($\mathrm{Re} = 1{\cdot}5 \times 10^4$) was investigated by Tokumaru & Dimotakis (1991). Their results indicate the possible attenuation of vortex shedding and the corresponding drag reduction by the rotary oscillations at much larger oscillation frequencies compared to the natural one. Later, the mechanism of resonance for the rotationally oscillating cylinder was investigated by Fujisawa *et al.* (1998), and the unsteady boundary layer over the cylinder was examined by Lee (1999). This type of control can be applied independent of the flow direction.

Berger (1967) introduced feedback control to the suppression of wake instability at low Reynolds numbers, using an oscillating body located in a low-turbulence air jet with the major axis aligned with the flow, whereas the feedback-sensor is located in the far wake. Natural vortex shedding occurred at Reynolds numbers above 77, but feedback control was able to prevent vortex shedding at Reynolds numbers up to 80. Later, Ffowcs-Williams & Zhao (1989) claimed the possible suppression of vortex shedding using acoustic feedback excitation. However,the results were reexamined by Roussopoulos (1993), who showed that they had misinterpreted their findings. Roussopoulos also found a delay in the onset of the wake instability and the spanwise locality of the control effect. On the contrary, the potential of feedback control at medium and high Reynolds numbers is very important from an engineering point of view and has been studied numerically by Fujisawa & Warui (1994) using cross-flow cylinder oscillations. The results have been confirmed by experiments by Warui and Fujisawa (1996). These observations indicate that the attenuation of vortex shedding is possible even for medium and high Reynolds numbers, and the control effect is mainly characterized by a phase lag and a feedback gain. However, the physical mechanisms of vortex-shedding attenuation have not been understood well.

The purpose of this paper is to experimentally study the feedback control of vortex shedding from a circular cylinder using rotary cylinder oscillations at medium Reynolds numbers. The flow response to this control is evaluated by measuring the mean and fluctuating velocities in the wake and the fluid forces on the cylinder. Moreover, the control mechanism is studied by measuring the pressure distributions over the cylinder surface as well as by visualizing the flow synchronized with the cylinder oscillations.

2. EXPERIMENTAL APPARATUS AND PROCEDURE

Figure 1 shows an illustration of the test-section and the velocity feedback mechanism employed in this study. The coordinate system is chosen in such a way that the x-axis is along the flow direction, the y-axis is in the vertical direction perpendicular to the flow, and the z-axis is in the spanwise direction, and the origin is located at the centre of the cylinder. The experiments are performed in a low-speed wind tunnel with a test-section of square cross-section, $0{\cdot}5\ \mathrm{m} \times 0{\cdot}5\ \mathrm{m}$ and $1{\cdot}5$ m long, providing a uniform velocity. A smooth circular cylinder of diameter $D = 100$ mm is positioned at the centre of the open test-section with two side walls, spanning the axis normal to the flow. To minimize the end-effects of the circular cylinder, two end-plates of radius 60 mm are fixed at the cylinder edges and the clearance between the wall and the end-plates is kept small but sufficient to allow smooth oscillations of the cylinder. The presence of the end-plates minimizes the leak flow through the clearance between the end-plates and the side-walls of the wind tunnel, which have been described by Warui (1996). Therefore, the spanwise distance between the end-plates is about 5 times of the cylinder diameter, which is about the same length as the spanwise correlation

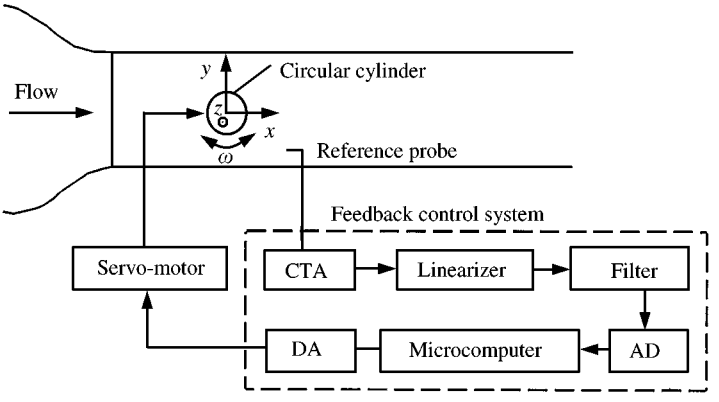

Figure 1. Experimental test-section and feedback control loop.

length of the sectional lift forces (Kacker *et al.* 1974). The influence of aspect ratio for stationary cylinder at around these Reynolds number is discussed by Szepessy & Bearman (1992) and Norberg (1994), who recommend the large aspect ratios over 20 for reaching a state independent of the end condition. The area blockage ratio of the cylinder to the cross-sectional area of wind tunnel is 0·2 in the present experiment. Although blockage affects the shedding frequency and the fluid forces on the cylinder to some extent (King 1977), the effect is not considered in the data analysis. The relatively low aspect ratio and the high blockage ratio of the cylinder in the present experiment are due to the limitation of the wind tunnel size and the frequency response of the AC servo motor used for controlling the cylinder oscillations. Therefore, the quantitative data may suffer from the influence of aspect ratio and blockage effect to some extent. Preliminary measurements indicate that the velocity distributions at the cylinder is uniform with an accuracy of 1% of the free-stream velocity in a spanwise distance of 400 mm and the free-stream turbulence is 0·8% of the free-stream velocity. Two hot-wires are positioned in the cylinder wake, one for detecting the feedback signal in lower shear layer for the control. The other one is for the measurement of mean and fluctuating velocities in the cylinder wake by traversing it in the flow field. The reference probe is located in the lower shear layer at $x/D = 1{\cdot}5$, $y/D = -0{\cdot}8$ and at the mid-plane $z = 0$ of the test-section, except for the cases otherwise noted.

The velocity signal $(U_r + u_r)$ at the feedback sensor is processed through a linearizer, a high-pass filter and a low-pass filter, which is fed to a microcomputer fitted with AD and DA converter (u_{rf}). The cut-off frequency of the high-pass filter is set to 1·6 Hz, while that of the low-pass filter is set to the Strouhal frequency of the vortex shedding. These filter settings allow the cylinder oscillation at the vortex-shedding frequency. A typical example of the gain and phase diagram of the filters is given in Figure 2, which corresponds to the experiments at $U = 1$ m/s. As the two filters interact near their cut-off frequencies, the signal gain at the shedding frequency (2·2 Hz) is reduced by 4 dB and the phase is delayed by 140°. These gain and phase characteristics which appeared in the filters are reflected in the estimation of feedback gain α $(= R\omega_{\max}/u_{rf\max})$ and phase lag ϕ in the controls, using the filter characteristics at the shedding frequency, where R is a radius of cylinder, $\omega_{\max}$ is a maximum angular velocity of the cylinder and $u_{rf\max}$ is a maximum of the filtered reference velocity. Here, the feedback gain α is defined as the ratio of the maximum circumferential velocity of the cylinder $R\omega_{\max}$ to the maximum of the filtered reference velocity $u_{rf\max}$ and the phase lag ϕ is the time lag in degrees between the filtered velocity signal (u_{rf}) and the monitored angular velocity signal (ω). The AC servo motor allows the

cylinder oscillations up to a frequency 8 Hz without significant phase lag between the input voltage and the measured angular velocity of the cylinder. However, the presence of the phase lag of the motor was considered in the data analysis. The phase-shift in the feedback controls is carried out with the program in the microcomputer by storing the digitized signal to a memory and taking out the previous data at several milliseconds from the memory, corresponding to the phase lag of the signal. The feedback signal is digitized every 2 ms, which is adjusted by a programmed timer in the program. The output signal from the DA converter (u_{rf}) is supplied to the AC servomotor. An example of the angular velocity signal and the filtered reference velocity signal is shown in Figure 3, which describes the definition of the phase lag ϕ in the control and the phase angle ϕ of the vortex shedding.

Measurement of mean and fluctuating velocities is carried out using a constant temperature anemometer with a temperature compensator. The hot-wire sensor is made of a tungsten wire of 5 μm diameter and 1 mm length. The overall accuracy of measurement is about $\pm 3\%$ for the mean and the fluctuating velocities, respectively. In order to obtain an insight into the flow mechanisms of the vortex formation and evolution, the flow field around the cylinder is visualized by smoke-wire method synchronized with the rotary oscillations of the circular cylinder. The observation is made by a CCD camera and the illumination is given by an argon-ion laser sheet of 3 W. The experimental details were

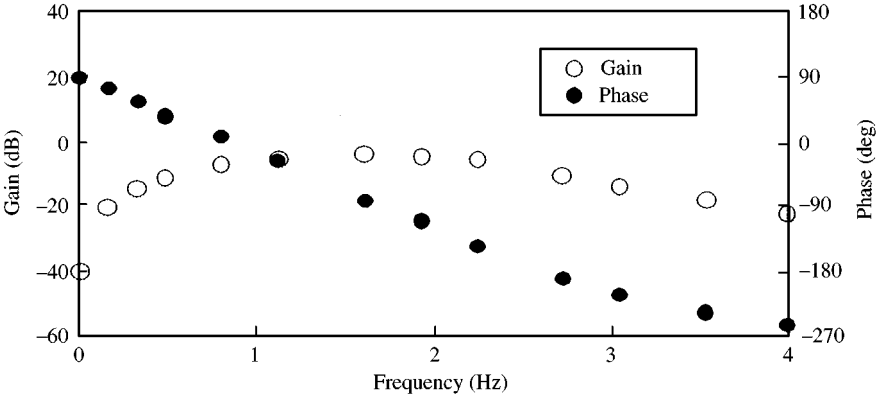

Figure 2. Phase and gain diagram of filters.

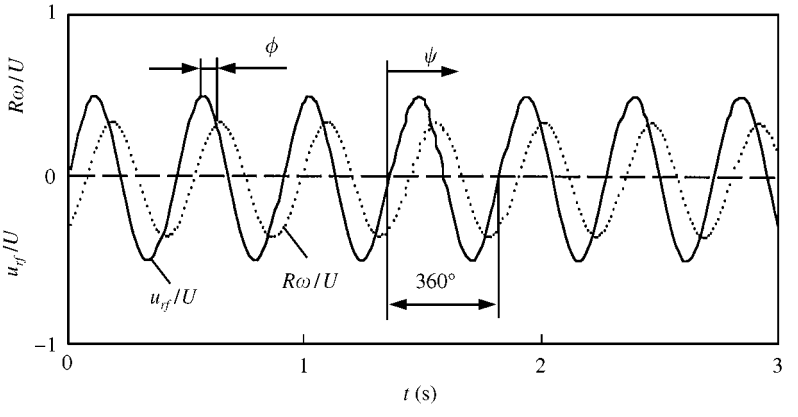

Figure 3. Definition of phase lag ϕ and phase angle ϕ of vortex shedding.

described by Fujisawa *et al.* (1998). These experiments are conducted at a flow velocity of 1 m/s, giving a Reynolds number $\mathrm{Re}(=DU/\nu) = 6{\cdot}7 \times 10^3$, where U is the uniform velocity of main flow and ν is the kinematic viscosity of fluid. The pressure distributions over the cylinder surface are measured by a pressure transducer of strain gauge type, which can detect the maximum pressure of 50 Pa. It is connected by a stainless-steel tube through a mechanical seal to a pressure hole over the cylinder surface. The experimental details and the data analysis are described by Fujisawa *et al.* (1998). This experiment is carried out at the free-stream velocity of $U = 3$ m/s, that is $\mathrm{Re} = 2 \times 10^4$, which is due to the experimental accuracy of the pressure measurement with the present pressure transducer.

3. RESULTS AND DISCUSSIONS

3.1. Response of Cylinder Wake to Feedback Controls

Figure 4 shows the effects of variation of the phase lag ϕ of the feedback control on (a) the mean and (b) the fluctuating velocities at the reference probe, and (c) the corresponding variations of maximum circumferential velocity of cylinder. The feedback coefficient α is set to 0·24, 0·48, and 0·96. It is seen that the mean and fluctuating velocity at the reference probe is influenced by the variations of the phase lag between the reference velocity signal and the cylinder oscillations. The mean velocities are increased and the velocity fluctuations are reduced around the phase lag $\phi = 240^\circ$. However, the mean velocities decrease and the velocity fluctuations increase at larger phase lags, such as $\phi = 380^\circ$ ($\alpha = 0{\cdot}24$), $\phi = 470^\circ$ ($\alpha = 0{\cdot}48$) and $\phi = 610^\circ$ ($\alpha = 0{\cdot}96$). The phase lag for minimizing the velocity fluctuations is referred to as the optimum phase and that for maximizing them is referred to as the reverse phase. Hence, the optimum phase is 240° and the reverse phase is 470° for $\alpha = 0{\cdot}48$. It should be mentioned that the velocity fluctuations at the optimum phase of $\phi = 240^\circ$ are smaller than those of the stationary cylinder, suggesting a possible attenuation of the vortex shedding by the optimum feedback control. A similar reduction in the velocity fluctuations also appears at phase lag of 600°, which is one cycle after the optimum phase, but the reduction is less than that for the optimum phase. Presumably the longer the phase lag, the smaller is the correlation between the reference signal and the vortex about to be shed from the cylinder. It is noted that the reverse phase lag, which corresponds to a phase lag at the maximum velocity fluctuations, increases as α increases, reflecting the decrease in the Strouhal frequency of rotationally oscillating cylinder with an increase in amplitude. This phenomenon has been observed by Fujisawa *et al.* (1998) and Baek & Sung (1998) for the rotationally oscillating cylinder under resonance condition, suggesting a similar control effect on the vortex shedding under the reverse-phase control and that under resonance. On the other hand, the maximum circumferential velocity of the cylinder responds in a similar way to the variations of the velocity fluctuations at the reference probe, but it increases gradually with the growth of feedback gain.

Figure 5 shows the variations of the mean and fluctuating velocities at the reference probe and the maximum circumferential velocity of cylinder with feedback gain α, under optimum-phase control at $\phi = 240^\circ$. The results for the stationary cylinder correspond to those shown at $\alpha = 0$ in this figure. It is clearly seen from this figure that the velocity fluctuations are reduced and the mean velocities are increased with an increase in feedback gain in a range of $\alpha = 0$–$0{\cdot}6$, which is opposite for larger feedback gain $\alpha \geq 0{\cdot}6$. This result indicates the presence of an optimum feedback gain for attenuating the velocity fluctuations at the reference probe by the present feedback control. On the contrary, the maximum circumferential velocity of cylinder gradually increases with α in the range of $\alpha = 0$–$0{\cdot}6$, and the growth rate becomes larger for further increases in α. It is noted that the maximum

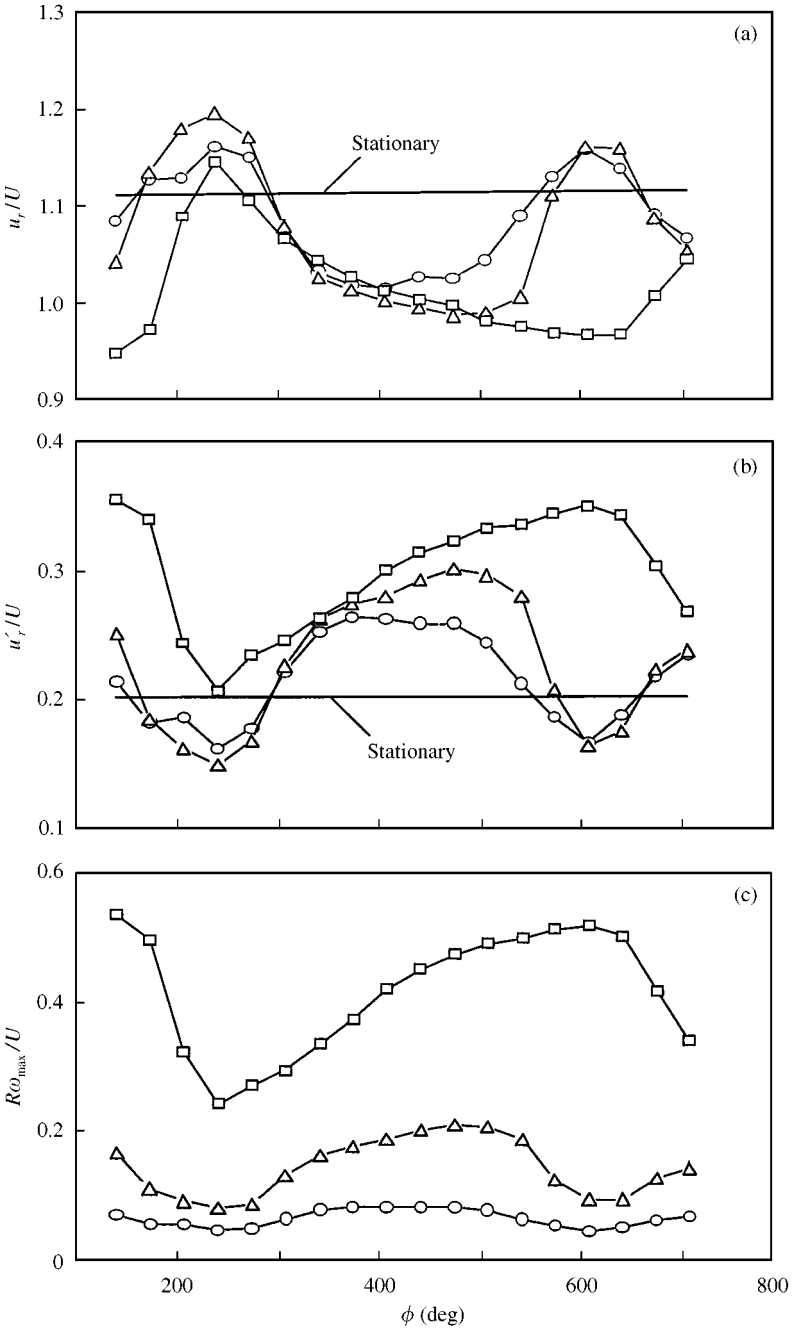

Figure 4. Response of reference velocities and cylinder motion to feedback controls ($Re = 6{\cdot}7 \times 10^3$). (a) Mean velocity; (b) fluctuating velocity; (c) circumferential velocity of the cylinder: ○, $\alpha = 0{\cdot}24$; △, $\alpha = 0{\cdot}48$, □, $\alpha = 0{\cdot}96$.

circumferential velocity of the cylinder at the optimum feedback control is about 10% of the free-stream velocity, where a reduction of 30% in the velocity fluctuations is produced in comparison with that for the stationary cylinder. The maximum half-angle of cylinder oscillation can be estimated by $\theta_{max} = \omega_{max}/(2\pi f)$, assuming a harmonic oscillation, where

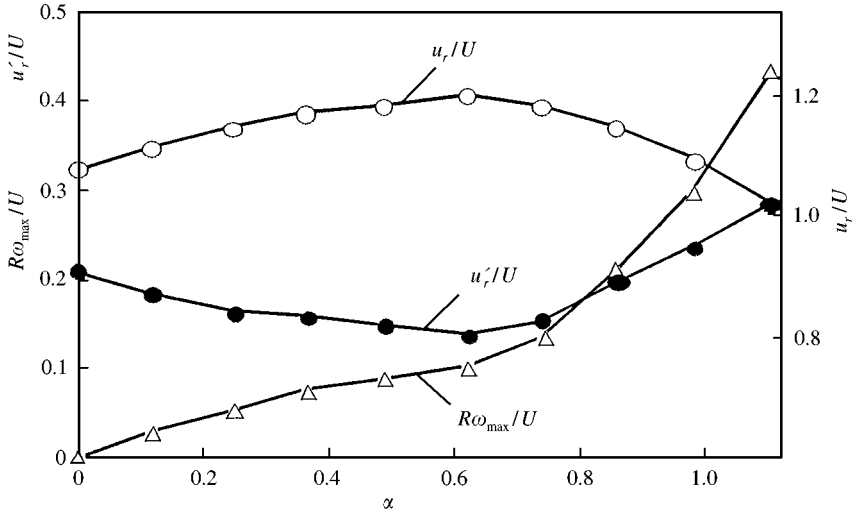

Figure 5. Effect of feedback coefficient α on flow and cylinder motion at optimum-phase control ($\mathrm{Re} = 6{\cdot}7 \times 10^3$).

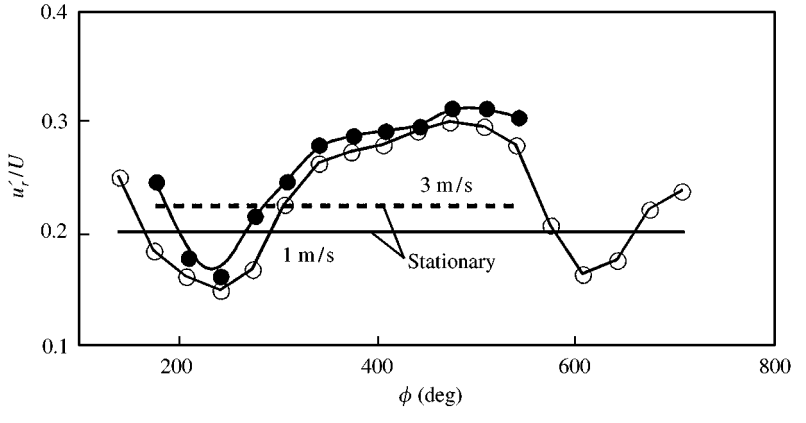

Figure 6. Response of fluctuating velocities to feedback controls at different free-stream velocities ($\alpha = 0{\cdot}48$): ○, $\mathrm{Re} = 6{\cdot}7 \times 10^3$; ●, $\mathrm{Re} = 2 \times 10^4$.

f is a frequency of cylinder oscillation. The maximum half-angle θ_{max} for optimum control is about 8°.

Figure 6 shows the response of fluctuating velocities at the reference probe to the feedback controls at a free-stream velocity of $U = 3$ m/s with a feedback gain of $\alpha = 0{\cdot}48$, which is compared with those at $U = 1$ m/s. Both results agree closely, and they indicate a decrease and an increase in fluctuating velocities at similar phase lags. This indicates that the optimum control parameters will be independent of the free-stream speed, and hence of Reynolds number, in the range of the present experiment.

3.2. Spanwise Variation of Control Effect

The spanwise variations of the control effect on the fluctuating velocities are measured by traversing a hot-wire probe in spanwise direction. The reference probe is fixed at $z/D = 1$ from the mid-plane of the test-section by keeping both probes at $x/D = 1{\cdot}5$ and

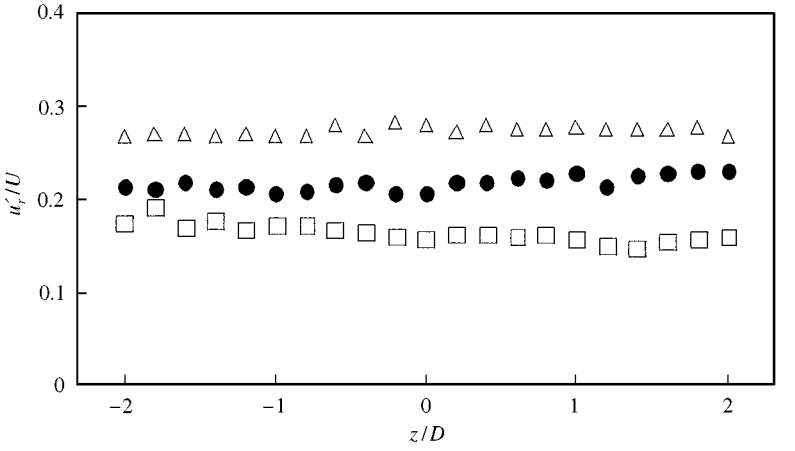

Figure 7. Spanwise variations of control effect on fluctuating velocities ($\alpha = 0{\cdot}48$, $\mathrm{Re} = 6{\cdot}7 \times 10^3$): ●, stationary; □, optimum phase; △, reverse phase.

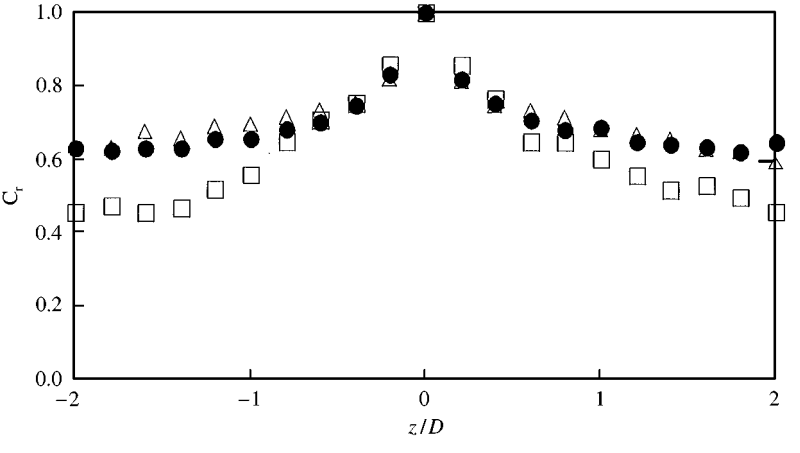

Figure 8. Spanwise distributions of correlation of fluctuating velocities ($\alpha = 0{\cdot}48$, $\mathrm{Re} = 6{\cdot}7 \times 10^3$): ●, stationary; □, optimum phase; △, reverse phase.

$y/D = -0{\cdot}8$. The measured velocity fluctuations under the optimum- and reverse-phase controls at feedback gain $\alpha = 0{\cdot}48$ are shown in Figure 7, which are compared with those of the stationary cylinder. Here, the velocity fluctuations at $z/D = 1$ are obtained from the reference probe. It is seen that the feedback control is effective over a considerable spanwise distance, which indicates that the flow properties are almost two-dimensional in the spanwise direction under feedback control.

Figure 8 shows the measurement of the cross-correlation coefficient Cr of the velocity fluctuations between the reference probe ($z/D = 0$) and the measuring probe at various spanwise locations by keeping the condition $x/D = 1{\cdot}5$ and $y/D = -0{\cdot}8$. The correlation coefficient shows a maximum value of 1 at the reference probe and it decreases gradually as the spanwise distance z increases. Comparing the correlation coefficients with that of the stationary cylinder, it is evident that the correlation coefficient for optimum-phase control is smaller than for the stationary cylinder. This corresponds to a breakdown of the spanwise correlation of vortex shedding by optimum-phase control, indicating the replacement of

the organized vortex streets by weakly irregular ones. This can be closely related to the observed reduction in velocity fluctuations in Figure 4(b). However, the correlation coefficient for reverse-phase control is merely increased as compared with that of the stationary cylinder. This result agrees qualitatively with the experiments of oscillating cylinder by Toebes (1969), who showed an increase in the spanwise correlation with the growth of the oscillation amplitude, accompanied by an increase in the drag coefficient. It should be taken into account that the spanwise distributions of velocity fluctuations in Figure 7 and the correlation coefficient in Figure 8 may suffer from unexpected effects related to the aspect ratio of the cylinder.

3.3. Distributions of Mean and Fluctuating Velocities

Figure 9 shows the distributions of the mean and fluctuating velocities measured in the cylinder wake at $x/D = 1{\cdot}5$ and $z = 0$ under optimum- and reverse-phase controls, respectively. The feedback gain α is set to an optimum value of 0·48. These are compared with those of the stationary cylinder. It is seen from the results that, under optimum-phase control, the mean velocity is increased outside the shear layer and is decreased near the cylinder center ($y = 0$), in comparison with the stationary cylinder. The opposite effect is

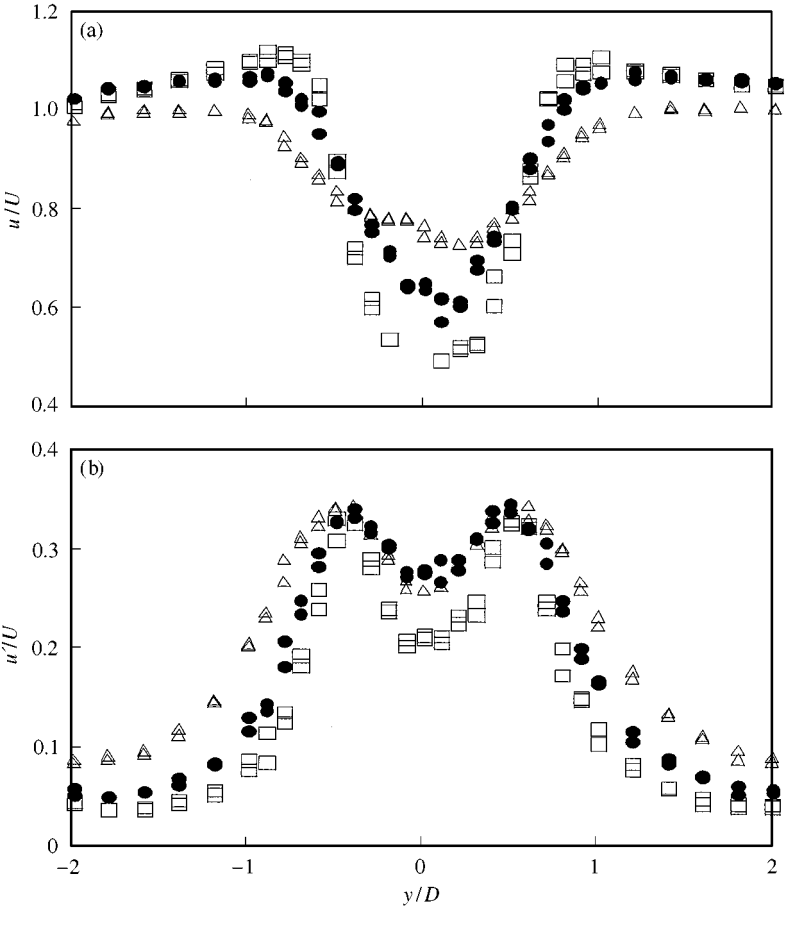

Figure 9. Distributions of mean and fluctuating velocities in cylinder wake ($x/D = 1{\cdot}5$, $\alpha = 0{\cdot}48$, $\mathrm{Re} = 6{\cdot}7 \times 10^3$): (a) mean velocity; (b) fluctuating velocity. ●, stationary; □, optimum phase; △, reverse phase.

observed for the reverse-phase control. Therefore, the wake width is decreased by the optimum phase control and is increased by the reverse-phase control. On the other hand, the measured distributions of velocity fluctuations are decreased in most of the wake region by the optimum control and they are increased by the reverse control, which also indicates the decrease and increase of wake width by the optimum and reverse-phase control, respectively. It is seen that the effect of active control is very strong at the shear layer ($y/D = -0{\cdot}8$) where the reference probe is located. However, the peak values of fluctuating velocities are only slightly reduced by the optimum-phase controls. These results agree qualitatively with the effect of the feedback controls by cross-flow cylinder oscillations as reported by Warui & Fujisawa (1996).

3.4. Power Spectrum

Figure 10 shows the measured power spectrum function Pu at the reference probe in relation to the frequency f (Hz) under optimum and reverse phase controls, which are compared with those of a stationary cylinder. Here the power spectrum function is defined as $\overline{u_r'^2} = \int_0^\infty Pu\mathrm{d}f$. The power spectrum is measured to determine changes in the turbulence structure and the turbulence energy distribution in the flow field when the rotational cylinder oscillation is feedback controlled. The power spectra are dominated by a principal peak at a frequency of 2·2 Hz corresponding to the Strouhal frequency of the stationary cylinder, which indicates the primary vortex-shedding frequency. A smaller peak occurs at double the frequency of the primary peak, indicating the effect of vortex shedding from the other side of the cylinder. The results show a reduction and enhancement of turbulence energy in some frequency ranges, especially around the peak spectrum by optimum- and reverse-phase controls, respectively, as compared with the stationary cylinder.

3.5. Pressure Distributions

Figure 11 shows the phase-averaged pressure distributions over the cylinder surface under feedback control (a) at the optimum phase and (b) at the reverse phase, which are compared

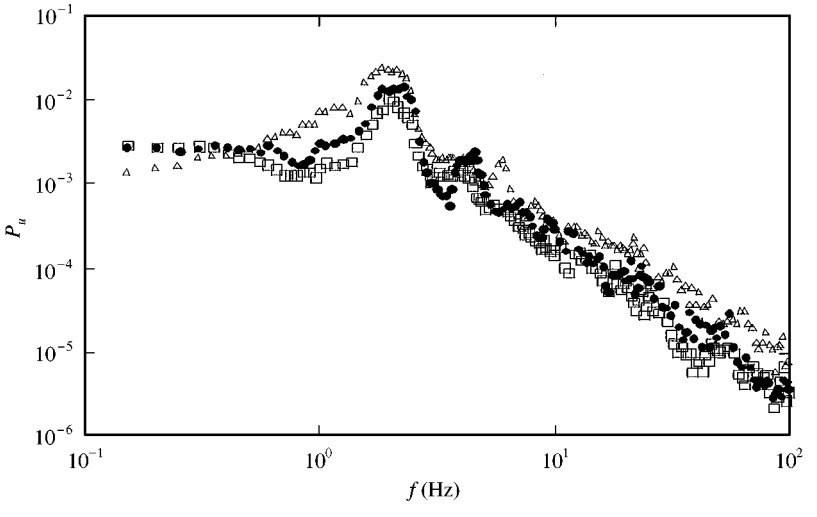

Figure 10. Power spectrum of reference velocity fluctuations ($\alpha = 0{\cdot}48$, $\mathrm{Re} = 6{\cdot}7 \times 10^3$): ●, stationary; □, optimum phase; △, reverse phase.

with (c) those for the stationary cylinder. Typical distributions of pressure coefficient $c_p = 2(p - p_\infty)/\rho U^2$ at four vortex phase angles $\phi = 0, 90, 180, 270^\circ$ are shown in this figure (p is the static pressure over cylinder surface, p_∞ the free-stream static pressure, and ρ the density of the fluid). It is noted that the magnitude of the pressure coefficient c_p is displayed over the cylinder, where $c_p = 1$ corresponds to the radius of the cylinder in this figure and ϕ is a phase angle of vortex shedding as defined in Figure 2. These four phase angles correspond to the acceleration phase, maximum, deceleration and minimum phase of the reference velocity signal, respectively. It is clearly seen that the variations of pressure patterns over the cylinder with the vortex phase angle ϕ under the feedback controls in (a) and (b) are similar to the stationary cylinder (c). However, the magnitude of pressure distributions is considerably modified by the feedback control effect. That is, the pressure distributions under optimum-phase control are reduced slightly and modified to be uniform over the cylinder surface except for the stagnation region. On the other hand, the pressure distributions under reverse-phase control are greatly enhanced to be asymmetrical, which indicates a large modification of flow pattern over the cylinder.

Figure 12 shows the phase- and time-averaged drag coefficient C_d under the feedback controls with the feedback gain $\alpha = 0{\cdot}48$, which is plotted against the phase lag ϕ in the controls. The drag coefficient is defined by $C_d = F_x/\rho U^2 R$ and is obtained by integrating the pressure distributions over the cylinder surface at the mid-plane ($z = 0$), where F_x is the streamwise force over a unit length of the cylinder. The results are obtained from the measurements over 800 shedding cycles. The results indicate a reduction and enhancement of the drag coefficient around optimum phase ($\phi = 240^\circ$) and reverse phase ($\phi = 470^\circ$), respectively. This variation of C_d with ϕ is very similar to that of the fluctuating velocities at the reference probe, which is shown in Figure 6. The results of these observations indicate that the fluid forces acting on the cylinder are well controlled by the optimized feedback loop with respect to the fluctuating velocities in the cylinder wake.

3.6. Flow Visualization of Vortex Formation

Figure 13 shows successive flow visualization pictures taken at four phase angles $\phi = 0, 90, 180, 270^\circ$ in a cycle of vortex formation for (a) the feedback control at the optimum phase, (b) at reverse phase, and (c) the stationary cylinder. The feedback gain is set at $\alpha = 0{\cdot}48$. The direction of cylinder rotation is shown by arrows in the pictures. The corresponding time variations of the filtered reference velocity u_{rf}/U and the circumferential velocity of cylinder $R\omega/U$ are given in the top diagrams, where ① corresponds to $\phi = 0^\circ$, ② to $\phi = 90^\circ$, ③ to $\phi = 180^\circ$, and ④ to $\phi = 270^\circ$ in the pictures, corresponding to the acceleration phase, maximum, deceleration and minimum phase of the reference velocity signal, respectively. It should be mentioned here that the magnitude of the filtered velocity signal is reduced by the optimum phase control and is enhanced by the reverse phase control in comparison with that of the stationary cylinder. This reduction by the feedback control agrees qualitatively with the measurement of velocity fluctuations in the wake and the fluid forces over the cylinder.

Examination of the flow pattern over the stationary cylinder in Figure 13(c) suggests that the lower shear layer receives a roll-up motion at $\phi = 270$ and 0°. This roll-up motion produces a low-pressure region at the lower surface of the cylinder, which has been observed in the measured pressure distributions as shown in Figure 11, suggesting the downward movement of the separation point over the cylinder surface. On the other hand, the relaxation of the lower shear layer is observed at $\phi = 90$ and 180°, which corresponds to the formation of high-pressure region over the lower cylinder surface and the upward movement of the separation point over the cylinder surface. Although a similar flow pattern in

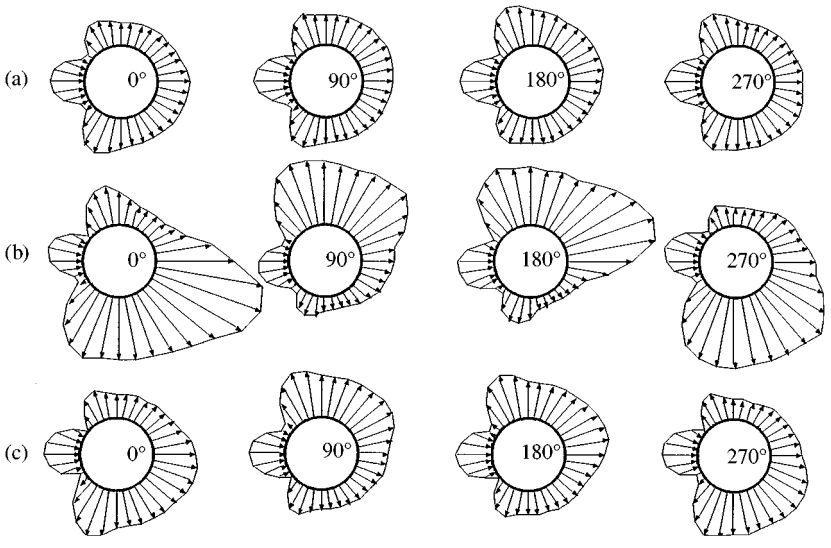

Figure 11. Phase-averaged pressure distributions over circular cylinder ($\alpha = 0{\cdot}48$, $\mathrm{Re} = 2 \times 10^4$): (a) optimum phase control; (b) reverse phase control; (c) stationary cylinder.

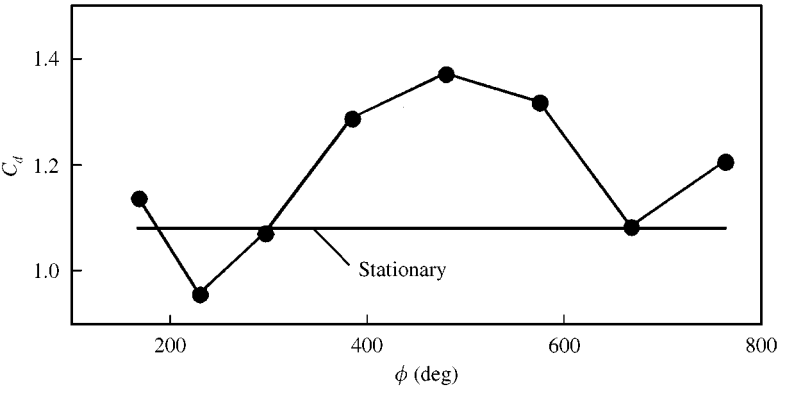

Figure 12. Response of phase- and time-averaged drag coefficient to feedback controls ($\alpha = 0{\cdot}48$, $\mathrm{Re} = 2 \times 10^4$).

a cycle of vortex formation is observed in the flow patterns under the feedback controls (a) and (b), the development of the wake and the strength of the roll-up motion are substantially modified by the effect of phase lags in the feedback controls. It is evident that the length of the wake region is elongated and the roll-up motion is weakened at the optimum phase; the opposite effect is observed at the reverse phase. These visualization results agree qualitatively with the attenuation and the enhancement of velocity fluctuations and fluid forces in the present measurement.

Detailed examination of the rotary motion of the cylinder and the corresponding flow patterns suggest the mechanisms of vortex attenuation and enhancement by the present active controls. In the case of feedback control at the optimum phase, the cylinder receives a counterclockwise rotation at $\phi = 270$ and 0°, as seen in the top diagram of angular velocity traces of the cylinder. (It is noted that the positive angular velocity of the cylinder corresponds to the counterclockwise rotation of the cylinder.) This cylinder motion is

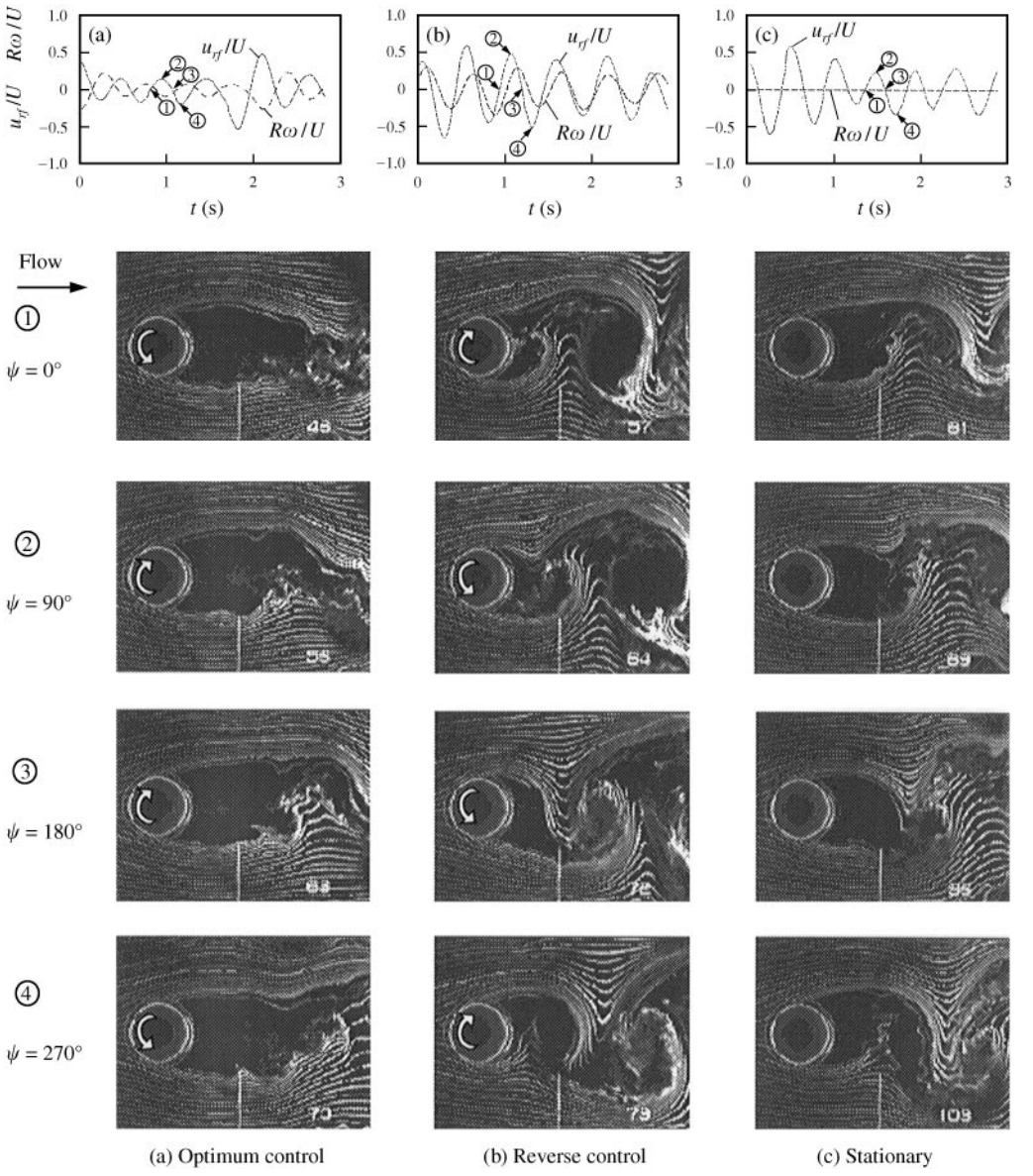

Figure 13. Simultaneous flow visualization synchronized with the cylinder oscillation ($\alpha = 0{\cdot}48$, $\mathrm{Re} = 6{\cdot}7 \times 10^3$). (The circled numbers at the left of the pictures correspond to those in the reference velocity traces.)

expected to reduce the magnitude of circulation over the lower side of the cylinder, because the velocity difference between the flow and the cylinder surface is decreased due to the counterclockwise rotation of the cylinder. Therefore, the attached flow observed at $\phi = 270$ and 0° is weakened by the cylinder rotation, as observed in the flow visualization picture under the optimum-phase control. The cylinder undergoes clockwise rotation at $\phi = 90$ and 180°, which promotes the injection of circulation from the lower side of the cylinder. Therefore, the time variations of the circulation produced from the shear layers are reduced and result in the attenuation of vortices as observed in the flow visualization pictures. On the other hand, the cylinder under reverse-phase control undergoes clockwise rotation at $\phi = 270$ and 0° and the counterclockwise rotation at $\phi = 90$ and 180°, which is opposite to the optimum-phase control. Therefore, the attached flow pattern over the cylinder surface and the relaxed pattern of the separated shear layer are promoted by the rotation effect of the cylinder and result in the strengthening of the roll-up motion of the vortices as observed in the flow visualization pictures. Thus, the vortices from both sides of the cylinder are dynamically attenuated by the feedback control at the optimum phase, and enhanced by the control at the reverse phase.

4. CONCLUSIONS

Experimental study of vortex-shedding control from a circular cylinder in a uniform flow is carried out using rotary cylinder oscillations controlled by a reference velocity signal in the wake. The results can be summarized as follows.

(i) An attenuation and an enhancement of the fluctuating velocities in the cylinder wake is observed in comparison with the stationary cylinder when the phase lag between the reference velocity and the cylinder oscillation is set to an optimum phase and a reverse phase, respectively. The reduction in the fluctuating velocities under optimum-phase control is maximized by optimizing the feedback gain.

(ii) The effect of feedback control on the flow field is studied by measuring the cross-sectional distributions of mean and fluctuating velocities, the spanwise distributions of fluctuating velocities and correlation, and the power spectrum. These results indicate the attenuation of the velocity fluctuations in the flow field and the reduction in the spanwise correlation by the optimum-phase control.

(iii) The phase- and time-averaged drag coefficient of the circular cylinder with and without feedback control is estimated by integrating the measured pressure distribution over the cylinder surface. The measurement under optimum-phase control indicates the reduction in the drag coefficients compared to the stationary cylinder, while it is clearly enhanced under the reverse phase control.

(iv) The simultaneous flow visualization synchronized with the cylinder oscillation indicates the mechanisms of vortex attenuation by optimum-phase control and enhancement by reverse-phase control, respectively. The vortex attenuation occurs at the optimum phase by successively cancelling the circulation and weakening the vortex formation by the effect of controlled cylinder oscillation, while the cylinder oscillation promotes the vortex formation under the reverse-phase control.

ACKNOWLEDGEMENTS

The authors would like to thank Prof. K. Nagaya, Mr S. Ikai of Gunma University and Miss R. Nishimagi of Niigata University for their helpful suggestions and cooperation to the present experiments.

REFERENCES

Baek, S. J. & Sung, H. J. 1998 Numerical simulation of the flow behind a rotary oscillating circular cylinder. *Physics of Fluids* **10,** 869–876.

Baz, A. & Ro, J. 1991 Active control of flow-induced vibrations of a flexible cylinder using direct velocity feedback. *Journal of Sound and Vibration* **146,** 33–45.

Bearman, P. W. 1984 Vortex shedding from oscillating bluff bodies. *Annual Review of Fluid Mechanics* **16,** 195–222.

Berger, E. 1967 Suppression of vortex shedding and turbulence behind oscillating cylinders. *Physics of Fluids* **10,** S191–S133.

Blevins, R. D. 1990 *Flow-Induced Vibration*, 2nd edition, pp. 43–103. New York: Van Nostrand Reinhold.

Ffowcs-Williams, J. E. & Zhao, B. C. 1989 The active control of vortex shedding. *Journal of Fluids and Structures* **3,** 115–122.

Filler, J. R., Marston, P. L. & Mih, W. C. 1991 Response of the shear layers separating from the circular cylinder to small amplitude rotational oscillations. *Journal of Fluid Mechanics* **231,** 481–499.

Fujisawa, N. & Warui, H. M. 1994 Active control of vortex shedding by cross-flow oscillation of a circular cylinder in a uniform flow. In *Proceedings of the Fourth FLUCOME*, Toulouse, France, pp. 113–118.

Fujisawa, N., Ikemoto, K. & Nagaya, K. 1998 Vortex shedding resonance from a rotationally oscillating cylinder. *Journal of Fluids and Structures* **12,** 1041–1053.

Griffin, M. & Hall, M. S. 1991 Vortex shedding lock-in and flow control in bluff body wakes. *ASME Journal of Fluids Engineering* **113,** 526–537.

Gunzburger, M. D. & Lee, H. C. 1996 Feedback control of Karman vortex shedding. *Journal of Applied Mechanics* **63,** 828–835.

Huang, X. Y. 1996 Feedback control of vortex shedding from a circular cylinder. *Experiments in Fluids* **20,** 218–224.

Kacker, S. C., Pennington, B. & Hill, R. S. 1974 Fluctuating lift coefficient for a circular cylinder in cross flow. *Journal of Mechanical Engineering Science* **16,** 215–224.

King, R. 1977 A review of vortex shedding research and its application. *Ocean Engineering* **4,** 141–172.

Lee, T. 1999 Investigation of unsteady boundary layer developed on a rotationally oscillating circular cylinder. *AIAA Journal* **37,** 328–336.

Norberg, C. 1994 An experimental investigation of the flow around a circular cylinder: influence of aspect ratio. *Journal of Fluid Mechanics* **258,** 287–316.

Okajima, A., Takata, H. & Asanuma, T. 1975 Viscous flow around a rotationally oscillating circular cylinder. *Reports of Institute of Space and Aeronautical Science, University of Tokyo*, No. 532, pp. 311–338.

Roussopoulos, K. 1993 Feedback control of vortex shedding at low Reynolds numbers. *Journal of Fluid Mechanics* **24,** 267–296.

Sarpkaya, T. 1979 Vortex-induced oscillations; a selected review. *Journal of Applied Mechanics* **46,** 241–258.

Szepessy, S. & Bearman, P. W. 1992 Aspect ratio and end plate effects on vortex shedding from a circular cylinder. *Journal of Fluid Mechanics* **234,** 191–217.

Taneda, S. 1978 Visual observations of the flow past a circular cylinder performing a rotary oscillation. *Journal of Physical Society of Japan* **45,** 1038–1043.

Toebes, G. H. 1969 The unsteady flow and wake near an oscillating cylinder. *ASME Journal of Basic Engineering* **91,** 493–505.

Tokumaru, P. T. & Dimotakis, P. E. 1991 Rotary oscillation control of a cylinder wake. *Journal of Fluid Mechanics* **224,** 77–90.

Warui, H. M. 1996 Experimental investigation on active control of vortex shedding from a circular cylinder by cross-flow oscillations. Ph.D. thesis, Gunma University.

Warui, H. M. & Fujisawa, N. 1996 Feedback control of vortex shedding from a circular cylinder by cross-flow cylinder oscillations. *Experiments in Fluids* **21,** 49–56.